Composition and temperature of Earth's inner core

Lars Stixrude[1] and Evgeny Wasserman[2]

Department of Earth and Atmospheric Sciences, Georgia Institute of Technology, Atlanta

Ronald E. Cohen

Geophysical Laboratory and Center for High Pressure Research, Carnegie Institution of Washington, D. C.

Abstract. We compare a theoretical prediction of the equation of state of iron at high pressures and temperatures to the properties of the Earth's inner core. The theoretical result is based on a first principles treatment of the static pressure and the pressure due to thermal excitation of electrons and an approximate ab initio (cell model) treatment of the vibrational pressure. The density of iron is found to be greater than that of the inner core even for unrealistically high temperatures of 8000 K. The isentropic bulk modulus of iron is found to be consistent with that of the inner core over a wide range of temperatures (4000–8000 K). We conclude on the basis of these comparisons that the inner core contains a substantial fraction of elements lighter than iron. Assuming ideal solutions, we find the temperature and light component mass fraction required to simultaneously match the density and bulk modulus of the inner core. For a temperature of 7000 K, 1 wt % O as FeO, satisfies the inner core observations. The temperature and mass fraction of S required depend on whether S is included as pyrite (2 wt % S, 5500 K) or as $Fe_{0.9}S$ (>8 wt % S, <3500 K). On the basis of this result and empirical mixing rules for Fe-O solutions, we argue that Fe-light element solid solutions at inner core conditions may be significantly nonideal. We derive expressions for the properties of nonideal multicomponent solutions that are valid in the limit of small amounts of impurities. These lead to general results for the properties of the alloy fraction that are required by comparisons of our equation of state of iron with seismological models.

1. Introduction

The composition and temperature of the Earth's inner core are of fundamental geophysical interest. The temperature of this central region provides a basic constraint on the thermal state and evolution of the planet. A great deal of attention has focused recently on determining the temperature at the inner core boundary, which is assumed to represent the equilibrium boundary between the solid inner core and the overlying liquid outer core. Equilibrium between these two regions has the important consequence that the composition of the inner core will reflect that of the much larger overlying liquid outer core from which it forms. Determination of the identity and amount of light element in the inner core would place important constraints on the earliest geochemical evolution of the Earth, especially of its siderophile fraction.

Major uncertainties remain, however. Estimates of the melting temperature of iron are currently uncertain by 30% [*Yoo et al.*, 1993; *Boehler*, 1993; *Williams et al.*, 1987]. Moreover, the uncertainty in the melting temperature of the core associated with the effect of the (unknown) light alloying element(s) is expected to be of comparable magnitude. Arguments based on geochemistry, or determinations of the properties of candidate alloys at high pressures and temperatures, have so far been

unable conclusively to rule out any of the oft-cited candidates for the light element in the core including O, S, H, Si, C, and others [*Jeanloz*, 1990; *Poirier*, 1994].

Most previous attempts to constrain the temperature and composition of the core have not dealt with the inner core itself. Estimates of the temperature have relied primarily on determinations of the melting point of iron and iron alloys at the inner core–outer core boundary, while estimates of core composition have focused primarily on comparisons with the properties of the liquid outer core. Here we take a different approach. We focus on the inner core because (1) its seismological properties, though somewhat more uncertain than those of the outer core, are known sufficiently precisely that they can place important constraints on the temperature and composition of the core and (2) the properties of solid iron are in principle better constrained and better understood at a fundamental level than are those of the corresponding liquid. The static equation of state of solid iron is measured to inner core pressures and the effects of temperature, including those due to the thermal excitation of phonons and electrons, can be accurately treated. Previous analyses of the temperature and composition of the inner core based on comparisons with seismological observations have relied on substantial extrapolations of the experimental equation of state of iron in pressure and temperature, based on semiempirical estimates of its thermodynamic properties [*Jephcoat and Olson*, 1987]. Moreover, previous analyses have focused only on the density of the inner core and have not compared the bulk modulus of iron alloys to that of the Earth.

We focus here on the properties of iron itself. We show that the equation of state of iron to the pressure-temperature con-

---

[1]Now at Department of Geological Sciences, University of Michigan, Ann Arbor.

[2]Now at Battelle, Pacific Northwest Laboratory, Richland, Washington.

ditions of the inner core is now well understood on the basis of first principles theoretical calculations that are independent of experiment yet explain existing static and dynamic compression data. Comparisons of the equation of state of iron with those of the inner core show that the inner core is less dense than iron but has a similar bulk modulus for plausible inner core temperatures. We conclude from these results that the inner core must contain a significant fraction of light elements.

2. Equation of State of Close-Packed Solid Iron

We assume that the solid phase of iron relevant to the inner core is close-packed. This is based on (1) the general notion that pressures in the inner core are large (more than twice the bulk modulus of iron) and will therefore favor efficiently packed phases and (2) detailed first principles calculations which show that non-close-packed phases are highly unfavorable energetically at inner core pressures and are unlikely to be thermodynamically stable. Indeed, the only phase other than fcc or hcp which has been seriously considered as the stable phase of iron in the inner core (bcc) is not only energetically unfavorable compared with fcc and hcp because of its lower density but is predicted to be mechanically unstable at high pressure [Stixrude and Cohen, 1995a].

Because we are dealing with only isotropically averaged properties in this study (density, bulk modulus), the precise structure of the close-packed phase is unimportant. First principles results show that fcc and hcp phases have nearly indistinguishable equations of state from 0 to at least 400 GPa [Stixrude et al., 1994]. Other close-packed phases, such as dhcp are also expected to have densities very similar to that of fcc or hcp. Although we will not deal with elastic anisotropy here, we note that the issue of the structure of the close-packed phase is all important in discussions of the seismic anisotropy of the inner core [Stixrude and Cohen, 1995b]. Elastic anisotropy may differ substantially even for phases such as fcc and hcp iron which have very similar bulk moduli. Indeed, the symmetry of the anisotropy in cubic and hexagonal phases is fundamentally different and the magnitude of the anisotropy is expected to be much greater in cubic phases.

The starting point for our ab initio description of the equation of state of iron is the division of the Helmholtz free energy of the system, $F(V, T)$, into contributions due to static compression, F_0, thermal excitation of electrons, F_{el}, and thermal excitation of phonons (vibrational contribution), F_{vib},

$$F(V, T) = F_0(V) + F_{el}(V, T) + F_{vib}(V, T). \quad (1)$$

The first two terms are calculated from first principles using the linearized augmented plane wave (LAPW) method [Stixrude et al., 1994]. The only essential approximation in these calculations is to the exchange-correlation potential, for which we use the generalized gradient approximation (GGA) [Perdew and Wang, 1992].

In general, the vibrational contribution is given by the partition function in the canonical ensemble, Z. Evaluation of this quantity requires an integration of a functional of the total energy over all vibrational degrees of freedom, an impossible task using a purely first principles approach. In order to treat the vibrational degrees of freedom, we make two approximations: (1) The total energy is evaluated with an approximate tight-binding total energy Hamiltonian [Cohen et al., 1994].

The parameters of this Hamiltonian are fit to accurate LAPW total energies and band structures of fcc, hcp, and bcc iron over a two-fold range of compression [Cohen et al., 1997]. The Hamiltonian reproduces the first principles results very precisely and is not expected to introduce any significant additional uncertainty in our calculations. (2) We approximate the partition function by assuming that the vibrations of atoms are uncorrelated. This mean-field approximation, known as the cell model [Holt and Ross, 1970; Holt et al., 1970; Ree and Holt, 1973; Westera and Cowley, 1975; Cowley et al., 1990], allows one to factorize the partition function so that the integral over all states is reduced to an integral over the coordinates of a single, so-called wanderer, particle within its Wigner-Seitz cell

$$Z_{cell} = \lambda^{-3N} \left\{ \int_\Delta \exp\left[-\beta(U(\mathbf{r}) - U_0)\right] d\mathbf{r} \right\}^N, \quad (2)$$

where k_B is Boltzmann's constant, h is Planck's constant, $\beta = (k_B T)^{-1}$, $\lambda = h/(2\pi m k_B T)^{1/2}$ is the de Broglie wavelength of the atoms, U_0 is the potential energy of the system with all atoms on ideal lattice sites, $U(\mathbf{r})$ is the potential energy of the system with the wanderer atom displaced by the radius-vector $\mathbf{r}$ from its equilibrium position, and N is the total number of atoms in the system. The integration is over the Wigner-Seitz cell, Δ, centered on the equilibrium position of the wanderer atom. The phonon contribution F_{vib} is then $F_{vib} = -k_B T \ln Z_{cell}$.

The cell model is applicable in the classical regime of interest here, between the Debye temperature and the melting temperature. It ignores diffusion and vibrational correlations. In this sense, it is similar to the Einstein model [e.g., Wallace, 1972], to which it reduces in the limit of small amplitude vibrations. However, unlike the Einstein approximation, anharmonicity, which is expected to be important at inner core temperatures, is accounted for. The neglect of diffusion and vibrational correlation is supported by our results which find that displacements comparable to the Wigner-Seitz radius do not contribute significantly to the integral (2), except at the highest temperatures and pressures of our study ($V < 50$ Bohr^3) (1 Bohr = 52.92 pm). At these extreme conditions, diffusion or correlated vibration may contribute a few percent to the thermal pressure (see below).

Thermodynamic quantities of interest, such as pressure and bulk modulus, are obtained by differentiating the Helmholtz free energy, for instance,

$$P = -(\partial F/\partial V)_T = P_{st}(V) + P_{el}(V, T) + P_{vib}(V, T) \quad (3)$$

Figure 1 plots these three contributions to the total pressure for iron along the Hugoniot. As one can see from Figure 1, the largest contribution is from static compression. Significantly, the static term (P_{st}), together with the other contribution that is evaluated purely from first principles, that due to thermal excitation of electrons, accounts for the largest part of the pressure ($>80\%$) even at inner core temperatures. The vibrational contribution is, however, not negligible, amounting to more than 50 GPa in the inner core.

Equation of state results for fcc and hcp iron using these methods have been reported previously [Wasserman et al., 1996]. For the purposes of this study, we have constructed simplified representations of our results which are valid over the range of volumes ($V = 45$–55 Bohr^3/atom) and temperatures ($T = 4000$–8000 K) of interest here. The representation is based on the completely general division of pressure

into a contribution from isothermal compression at a reference temperature, T_R, and a thermal part,

$$P(V, T) = P(V, T_R) + \int_{T_R}^{T} \alpha K_T \, dT', \tag{4}$$

where $\alpha K_T = (\partial P/\partial T)_V$ is in general a function of volume and temperature [Anderson, 1995].

For iron, we have found that αK_T is nearly independent of volume at high pressure and that it depends approximately linearly on temperature [Wasserman et al., 1996]. This behavior contrasts with that of insulators [Anderson, 1995] and originates in the electronic contribution to the thermal pressure. We constructed a linear fit to our results at $V = 55$ Bohr^3,

$$\alpha K_T = a_0 + a_1(T - T_R), \tag{5}$$

which leads to the thermal pressure

$$P_{TH} = a_0(T - T_R) + \tfrac{1}{2}a_1(T - T_R)^2. \tag{6}$$

The thermal pressure determined from the cell model begins to show a slight volume dependence at the highest densities ($V < 50$ Bohr^3) and temperatures of our study. An examination of the wanderer potential $U(r)$ under these conditions indicates that the deviation is not intrinsic to the system but is rather due to a breakdown of the cell model approximation; displacements comparable to the Wigner-Seitz radius begin to contribute significantly to the integral. Nevertheless, the effect is small: the maximum deviation between cell model results and the representation (5 and 6) is 6% in P_{TH} over the pressure regime of the inner core.

The isotherm at the chosen reference temperature $T_R = 4000$ K was fit to a finite strain-like expansion in $V^{-2/3}$

$$P(V, T_R) = m_0 + m_1 V^{-2/3} + m_2 V^{-4/3}. \tag{7}$$

The isothermal bulk modulus, $K_T = -V(\partial P/\partial V)_T$, is calculated by differentiating (7). The isentropic bulk modulus K_S is obtained from the thermodynamic identity
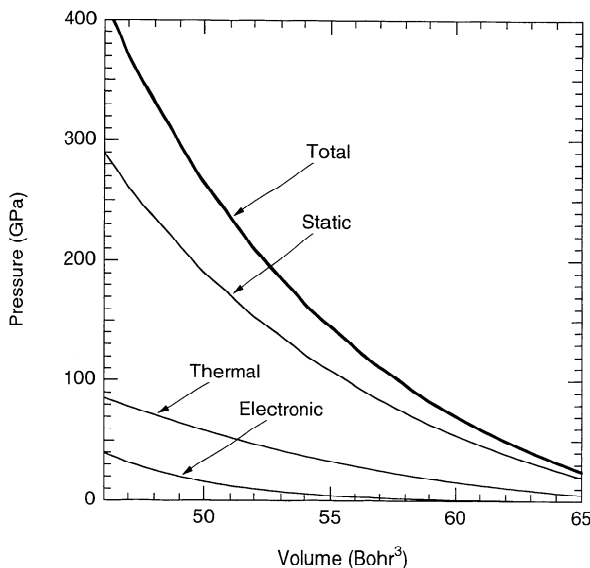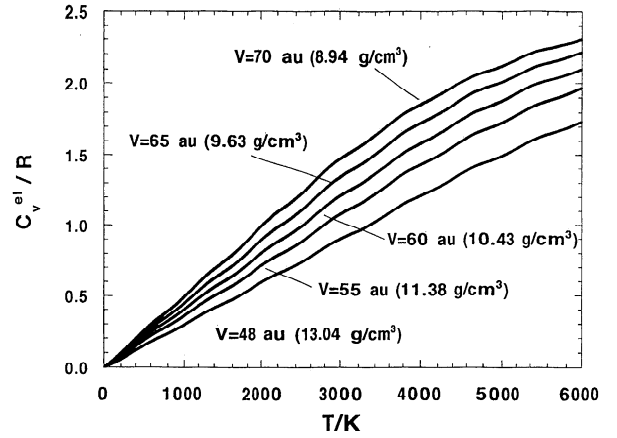

Figure 2. Calculated electronic contribution to the constant volume heat capacity for pure iron. The calculations are represented by (10) for temperatures 3000–8000 K and $V = 45$–55 Bohr^3/atom (au = atomic unit = Bohr^3/atom).

$$K_S = K_T(1 + \alpha\gamma T), \tag{8}$$

where the thermal expansivity was determined as $\alpha = (\alpha K_T)/K_T$ and the Grüneisen parameter from

$$\gamma = \alpha K_T V/C_V, \tag{9}$$

where C_V is the isochoric heat capacity. We find that the Grüneisen parameter depends significantly on temperature at high pressure, violating the usual quasi-harmonic approximation. The temperature dependence originates in the electronic contributions to αK_T and the heat capacity.

In order to complete the thermodynamic description and to be able to calculate the isentropic bulk modulus, one needs the volume and temperature dependence of C_V. The lattice heat capacity was assumed to be $3R$, R being the universal gas constant. As we demonstrated before [Wasserman et al., 1996], at the density-temperature regime of the core the deviation of the lattice heat capacity from $3R$ is much less than the electronic heat capacity and can therefore be neglected without introducing a significant error.

The electronic heat capacity C_V^{el} was calculated under the assumption that coupling between thermal excitation of electrons and phonons is negligible. The temperature dependence of the calculated C_V^{el} is given in Figure 2. The results of our calculations are in good agreement with the study of Boness et al. [1986]. For the purpose of this study, C_V^{el} was calculated on a dense mesh of temperatures from 3000 K to 8000 K and volumes ranging from 45 to 55 Bohr^3/atom and interpolated with a least squares polynomial

$$C_V^{el} = \sum_{i=0}^{1} \sum_{j=1}^{3} c_{ij} V^i T^j. \tag{10}$$

This polynomial approximation was found to be entirely satisfactory over the range of interest: deviations from the calculated electronic heat capacity are no more than 1.0%. Though temperatures less than 3000 K are not of interest here, we note that the polynomial has the correct low-temperature limiting form, and it can be extrapolated to temperatures lower than 3000 K with relative error of 3%. This result may be useful in reducing shock wave data. The coefficients appearing in (5)–(7), and (10) are given in Tables 1 and 2.

Figure 1. Contributions to pressure along the Hugoniot (1 Bohr = 52.92 pm).

Table 1. Fit Parameters for the Equation of State of Close-Packed Iron (Equations (5)–(7))

Parameter	Value
m_0	1431.6 GPa
m_1	$-53,395$ GPa Bohr^2
m_2	506,065 GPa Bohr^4
a_0	12.96 MPa K^{-1}
a_1	7.8 kPa K^{-2}

One Bohr = 52.92 pm.

3. Estimate of Uncertainties

Our calculation of the equation of state of iron at pressures and temperatures of the inner core involves several levels of approximation. The degree of accuracy of these approximations differs considerably for the three contributions to pressure, namely, static pressure, contribution due to thermal excitations of electrons, and that of phonons. Fortunately, the largest contribution, that due to static compression, is evaluated most accurately. In this section we estimate the accuracy of our equation of state and provide a conservative estimate of the probable error.

The LAPW calculations that are used to calculate the static pressure and the pressure due to thermal excitation of electrons involve one serious approximation, the generalized gradient approximation (GGA) to the exchange-correlation potential. We estimate the error in this approximation by comparing our theoretical static equation of state to the experimentally determined one at room temperature. The standard deviation in pressure of the athermal calculations of Stixrude et al. [1994] from the experimental measurements of Mao et al. [1990] is less than 10 GPa for the density range of interest (Figure 3). (Deviations are larger at low pressures; this may be due to magnetic contributions, which are unimportant at high pressures, and are neglected here.) Adding zero point motion and 300 K thermal pressure to the LAPW results improves agreement with experiment. The relative error in the pressure due to thermal excitation of electrons is more difficult to estimate but is likely to be comparable to that in the static pressure. Under this assumption, uncertainties in P_{el} would add an additional uncertainty of less than 1 GPa which is small compared to the absolute uncertainty in the static pressure alone.

Calculation of the vibrational pressure involves two approximations: the tight-binding Hamiltonian and the cell model. The well-known agreement between the Einstein model, a special case of the cell model, and a variety of high-temperature experimental data indicates that the errors incurred by the cell model approximation are not likely to be large [Wallace, 1972]. We can make a quantitative, if indirect, evaluation of the likely error by comparing to calculations on the fcc argon, for which cell model results may be compared with essentially exact Monte Carlo evaluations of the partition function [Cowley et al., 1990]. The discrepancy between cell model and Monte Carlo results is no more than 3% up to temperatures 10 times that of the Debye temperature. If we allow for an additional uncertainty of 6% to account, conservatively, for possible errors in the representation of the thermal pressure (6), we find an error of 9%, or 5 GPa in the vibrational pressure for the conditions of the inner core.

The total uncertainty in our equation of state then is of the order of 16 GPa over the density range of interest. This cor-

responds to a relative uncertainty in pressure of 5% and an uncertainty in density of 0.16 Mg m^{-3} or 1%. We can independently evaluate this estimate of uncertainty by comparing theory with the experimentally measured room temperature equation of state and the density, bulk sound velocity, and Grünseisen parameter measured along the Hugoniot (Figure 3). The maximum deviation of the calculations from the solid-phase portion of the experimental Hugoniot at core pressures is less than 5 GPa, less than half of our estimated uncertainty, consistent with our estimate being a conservative one. The maximum deviation between theoretical and experimental bulk sound velocity is 3%. Comparisons with other experimental results are reported by Wasserman et al. [1996].

4. Comparison With the Inner Core

We compare our equation of state of iron to the properties of the inner core as determined seismologically. For the first time, we compare to not only the density of the inner core but also its bulk modulus. This is significant as the comparison with two properties places greater constraints on the possible composition and temperature of the inner core. We will assume for the purposes of these comparisons that the inner core is isothermal. We support this assumption below by analyzing the thermal state of the inner core and provide further support for our contention that the inner core is not likely to be composed of pure iron.

The density profile of the inner core is compared with isotherms of pure iron calculated with our equation of state in Figure 4a. For temperatures in the middle of the range typically estimated for the inner core (6000 K) the density of iron is 3% greater than that of the inner core. This difference lies outside the combined uncertainties in our equation of state and in the seismological models [Masters and Shearer, 1990]. We note that even for temperatures as high as 8000 K, somewhat higher than the highest estimates of inner core temperatures, iron is still slightly denser than the inner core.

We find that temperatures in excess of 8000 K are required for the density of iron to coincide with that of the inner core. The conclusion that very high temperatures are necessary is consistent with previous results, although the requisite temperatures found here are somewhat higher than those found by Jephcoat and Olson [1987]. They found that a temperature of 7000 K was adequate to yield agreement between the equation of state of iron and the inner core. The differences between our result and theirs are due to the different equations of state used. Because of the limited experimental data then available, Jephcoat and Olson were forced to extrapolate their semiempirical equation of state well outside the range of measure-

Table 2. Coefficients of the Polynomial Approximation for the Electronic Heat Capacity of Close-Packed Iron (Equation (10))

Coefficient	Value
c_{01}	-0.273×10^{-03}
c_{02}	0.552×10^{-07}
c_{03}	-0.119×10^{-11}
c_{11}	0.115×10^{-04}
c_{12}	-0.884×10^{-09}
c_{13}	-0.150×10^{-13}

The volume is in units of Bohr^3/atom, temperature in kelvins, and C_V^{el} is in units of the universal gas constant R.
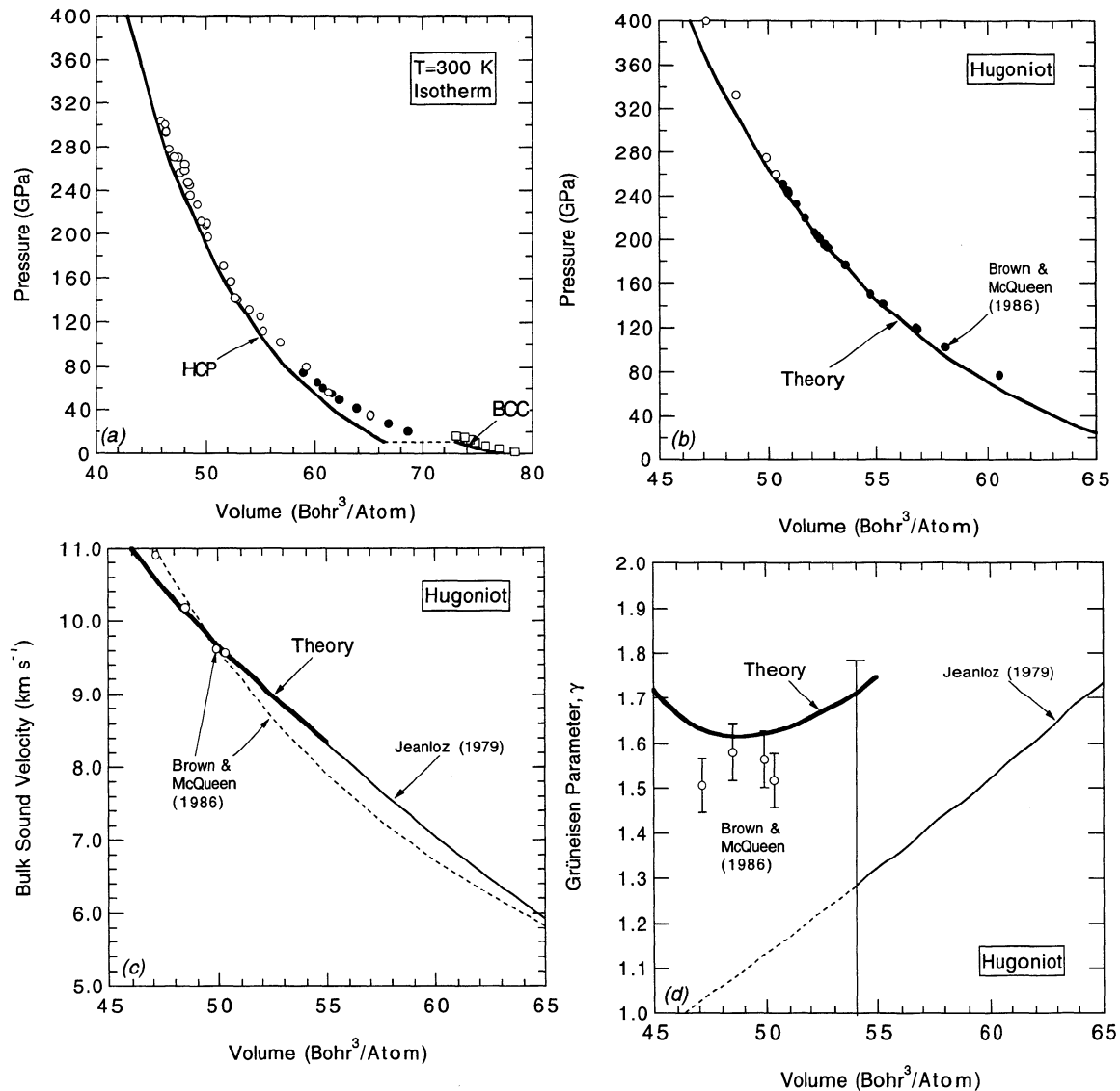
Figure 3. Theoretical prediction compared with experimental measurements of iron. (a) The low-temperature equation of state: theory, lines; experiments, squares and solid circles [*Jephcoat et al.*, 1986] and open circles [*Mao et al.*, 1990]. Dashed line indicates the theoretically predicted bcc-hcp transition pressure (11 GPa). (b) The Hugoniot: theory, line; experiment, solid circles are solid phase and open circles are liquid phase. (c) Bulk sound velocity along the Hugoniot: theory, bold line; experiment, light line and open circles. Dashed line is the fit of *Brown and McQueen* [1986] to their data. (d) Grüneisen parameter: theory, bold line; experiments, light line, dashed extrapolation, large error bar [*Jeanloz*, [1979] and symbols [*Brown and McQueen*, 1986].

ments. They also did not include an explicit division of vibrational and electronic thermal pressures. In any case, in the absence of independent estimates of the temperature of the inner core, comparisons based on the density alone cannot constrain the composition of the inner core. It is clearly possible to find inner core temperatures (albeit higher than all previous estimates, i.e., $T > 8000$ K) such that pure iron provides an acceptable match to the density of the inner core.

The isentropic bulk modulus of the inner core is compared with that of iron calculated with our equation of state in Figure 4b. The isentropic bulk modulus of iron depends weakly on temperature and is very close to that of the inner core for temperatures ranging from 4000 to 8000 K. We have found that the temperature which produces the best fit between the

bulk modulus of iron and the inner core is 7000 K. At 6000 K the maximum deviation between iron and seismological models of the inner core is 2%.

We have also compared our results to the larger number of seismological models which are parameterized only in terms of V_P and V_S, the P and S wave velocities of the inner core, by examining the bulk sound velocity V_B (Figure 4c),

$$V_B = \sqrt{K_S/\rho} = \sqrt{V_P^2 - \tfrac{4}{3}V_S^2}.$$

Because the bulk modulus of pure iron is comparable to that of the inner core, and its density higher, the bulk sound velocity of iron does not match that of the inner core even for the highest temperatures we examined (8000 K). The maximum
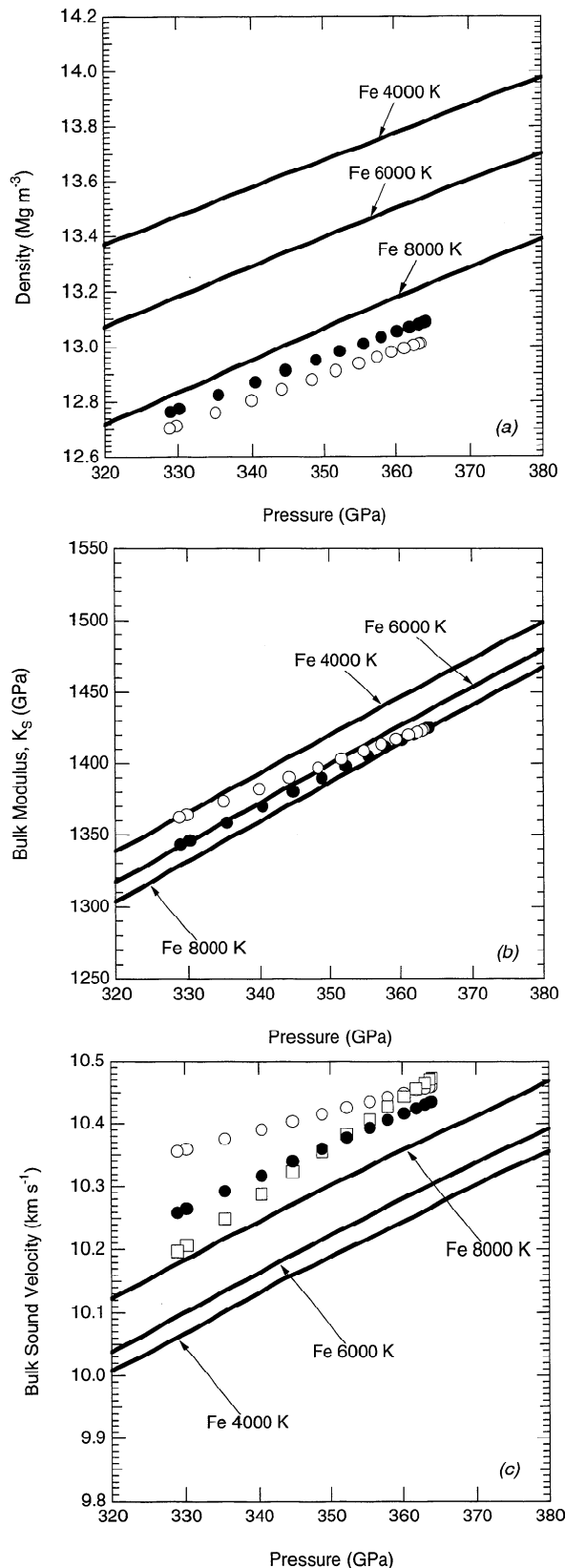
Figure 4. Properties of pure iron along three isotherms (solid lines) compared with those of the inner core (a) density (b) isentropic bulk modulus, and (c) bulk sound velocity. The properties of the inner core are represented by the seismological models of *Dziewonski and Anderson* [1981] (solid circles); *Dziewonski et al.* [1975] (open circles); and *Morelli and Dziewonski* [1993] (squares).

difference between V_B of iron at 6000 K and that of the inner core is 3%.

Our comparisons show that it is possible to find inner core temperatures such both the density and bulk modulus of iron match that of the inner core within the combined uncertainties of theory and seismological models ($T = 8000$ K). This temperature is higher than most estimates of the temperature of the inner core. If the temperature is significantly less than 8000 K, our analysis indicates that a significant fraction of lighter elements is present in the inner core.

5. Thermal State

Here we justify our assumption that the inner core is approximately isothermal and provide an independent estimate of its temperature. We can estimate a probable upper bound on the temperature gradient in the inner core by assuming that it is perfectly insulating. If the inner core grows through freezing of the overlying outer core, its temperature profile will then directly reflect the solidus temperature. We estimate the depth dependence of the solidus temperature T_s using the Lindemann law

$$\partial \ln T_s / \partial \ln \rho_s = 2(\gamma_{lat} - 1/3), \qquad (11)$$

where ρ_s is density of the solid at T_s and γ_{lat} is the lattice Grüneisen parameter, the phonon contribution to γ. Assuming that the inner core is in hydrostatic equilibrium and neglecting the depth dependence of density and bulk modulus,

$$T_s(r) = T_s(0) \exp\left[\frac{\Gamma\Pi}{K}\left(\frac{r}{c}\right)^2\right], \qquad (12)$$

where r is radial distance, c is the radius of the inner core, $\Gamma = 2(\gamma_{lat} - 1/3)$, and $\Pi = 2\pi G\rho^2 c^2/3$ is the pressure due to the inner core's self-gravitation. We find that γ_{lat} varies somewhat over the pressure range of the inner core and over the range of previous estimates of the temperature of the inner core. However, it is well approximated by the value 1.6 for the purposes of estimating the temperature gradient. Taking $K = 1400$ GPa and $\rho = 13$ Mg/m^3 and evaluating (12), for a central temperature of 6000 K we find that the temperature difference across the inner core is less than 400 K.

Conductive or convective heat loss will decrease the temperature difference across the inner core relative to the insulating case. For example, if the inner core is convecting [*Jeanloz and Wenk*, 1988], its temperature distribution will be adiabatic. The temperature gradient is then given by (12) with $\Gamma = \gamma$. The thermodynamic Grüneisen parameter γ is a weighted average of γ_{lat} and the electronic contribution γ_{el}. We have found in our ab initio results that $\gamma \approx \gamma_{lat} \approx \gamma_{el}$. Then, the adiabatic temperature difference is less than that in the insulating case by a factor $2[1 - (3\gamma)^{-1}]$, or ~250 K. Plausible amounts of radioactive heat production, H, in the inner core are unlikely to change these estimates substantially. Even if H is 10 times the bulk Earth value (2.5×10^{-8} W m^{-3} [*Verhoogen*, 1980]), the superadiabatic steady state temperature drop across the inner core, for a conductivity of $k = 100$ W m^{-1} K^{-1}, is only 60 K [*Jeanloz and Wenk*, 1987]. We conclude that the temperature difference across the inner core is small; the variation in ρ and K over the estimated temperature range is smaller than uncertainties in our theoretical calculations and in the seismological models. It is then sensible to assume that the inner core

is isothermal for the purposes of comparing theoretical and seismological equations of state.

We can estimate an upper bound to the temperature at the inner core boundary on the basis of our ab initio results in the following way. We assume that the core solidus lies below the melting point of pure iron. Our estimate of the melting temperature of iron is based on our calculation of the temperature along the Hugoniot. We find that the Hugoniot temperature at the melting pressure of 243 GPa [*Brown and McQueen*, 1986], is $T_{sH} = 5600$ K [*Wasserman et al.*, 1996]. Our result agrees well with the estimates of *Brown and McQueen* [1986] and *Bonness and Brown* [1990] and is ~800 K less than that measured by *Yoo et al.* [1993]. The difference in density between the Hugoniot melting pressure and the pressure at the inner core boundary (329 GPa) is small (4%). We may then perform a short extrapolation to find the melting temperature of iron at the inner core boundary using the Lindemann law (12) [*Brown and McQueen*, 1986]. For the melting temperature of iron at the inner core boundary we obtain

$$T_{sICB} = T_{sH}(\rho_{ICB}/\rho_{sH})^{2(\gamma_{lat}-1/3)} = 6150 \text{ K}, \qquad (13)$$

where ICB quantities are those at the inner core boundary, and H quantities are those at the conditions of melting along the Hugoniot, and we have used $\rho_{ICB} = 12.76 \text{ Mg m}^{-3}$ [*Dziewonski and Anderson*, 1981], $\rho_{sH} = 12.30 \text{ Mg m}^{-3}$ and $\gamma_{lat} = 1.6$ [*Wasserman et al.*, 1996]. This estimate of the upper bound of the inner core boundary temperature agrees with that of *Brown and McQueen* [1986] and is unlikely to be in error by more than 1000 K on the basis of the estimated uncertainties in our equations of state and comparison with independent experimental results. This estimate is significant because it means that a pure iron composition for the inner core can now be ruled out on the basis of a comparison with the density alone. At a temperature of 6150 K the density of pure iron is 0.37 Mg m^{-3} or 3% greater than that of the inner core.

6. Light Element in the Inner Core

The discrepancy between the properties of pure iron along probable geotherms and the inner core is most likely caused by the presence of additional, lighter elements. Major questions include the identity (O, S, H, etc.) and amount of light element in the inner core. It is likely that more than one element besides iron exists in substantial quantities in the inner core, not all of which need be lighter than iron. For example, Ni is expected to be present in the inner core on the basis of its association with iron in meteorites.

Current geophysical observations and laboratory measurements of the equations of state of candidate alloying components cannot rule out conclusively any of the large number of light alloying elements which have been proposed on geochemical grounds. In particular, although important advances are being made in the determination of the equation of state of Fe-O Fe-S, Fe-H, and Fe-Si alloys, these are not yet of comparable precision to our knowledge of the iron equation of state. Moreover, theoretical predictions of the high pressure-temperature equations of state of these alloys complementary to our results for iron do not yet exist.

6.1. Approach

Because of the uncertainty in the identity of the alloying elements in the core and the material properties of candidate alloying components, it is not yet possible to place definite limits on the amount of elements other than iron in the inner core. The approach we take here is to identify the material properties that the alloying fraction must have in order to satisfy, when combined with our equation of state of iron, the properties of the inner core [*Jeanloz*, 1979]. Unlike previous approaches, we do not assume that the solution is binary or that mixing is ideal.

To proceed, we assume that the inner core consists of a solid solution, rather than a mechanical mixture of two or more phases. The formation of solid solutions, at least over limited ranges of composition, is expected on general grounds at the high temperatures of the inner core. Solvi may exist, but we assume that they occur outside the relatively narrow compositional range of interest here, i.e., less than 10 wt % or 20 mol % light elements.

As our starting point, we take the following general expression for the Gibbs free energy of a binary solution consisting of Fe (component 1) and other components ($2, \cdots, N$):

$$G = \sum_{i=1}^{N} x_i[G_i + RT \ln f_i x_i], \qquad (14)$$

where x_i are the mole fractions of the end-member components, G_i are their Gibbs free energies, R is the gas constant, and f_i are the activity coefficients. The volume is the derivative of G with respect to P at constant T and composition

$$V = \sum_{i=1}^{N} x_i V_i + V_{mix}(\mathbf{x}), \qquad (15)$$

where all nonideal volume terms are contained in V_{mix} which depends on the composition vector $\mathbf{x}$,

$$V_{mix}(\mathbf{x}) = RT \sum_{i=1}^{N} x_i \left(\frac{\partial \ln f_i}{\partial P} \right)_{T,\mathbf{x}}. \qquad (16)$$

If the solution is ideal ($f_i = 1$, all i), or if the activity coefficients depend only weakly on pressure over the range of interest, V_{mix} is negligible.

Since we are interested in nearly pure iron solutions, we expand V_{mix} in a Taylor series about $x_1 = x_{Fe} = 1$,

$$V = x_{Fe}V_{Fe} + \sum_{i=2}^{N} x_i \hat{V}_i + O(x_i^2), \qquad (17)$$

where

$$\hat{V}_i = V_i + (\partial V_{mix}/\partial x_i)_{x_1=1}. \qquad (18)$$

This result is significant because it shows that to lowest order in the light element concentrations, the volume may be treated as that of an ideal solution but one where the partial molar volumes of the light components are replaced by the volumes of virtual (fictive) components ($\hat{V}_i$). The volumes of these virtual components can be thought of as effective partial molar volumes which account for the effects of the nonideal volume of mixing. The difference between the volume of a component and its virtual counterpart will be large to the extent that nonideal effects are important (Figure 5). It is worth pointing out that (17) is in essence a restatement of Henry's law.

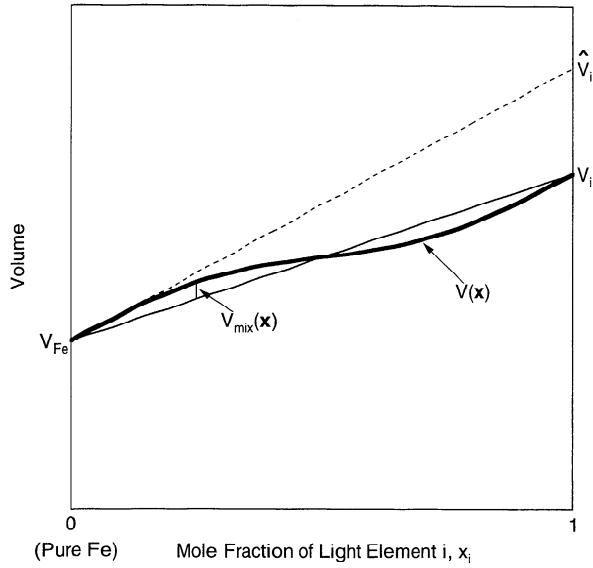The density and bulk modulus of the solution are given by

Figure 5. Schematic illustration of the difference between the molar volume of an alloying component (V_i) and its virtual counterpart ($\hat{V}_i$) in a nonideal solution where the volume of mixing is significant.

$$\rho^{-1} = (1 - m)\rho_{Fe}^{-1} + m \sum_{i=2}^{N} \frac{m_i}{m} \hat{\rho}_i^{-1} \tag{19}$$

and

$$(\rho K)^{-1} = (1 - m)(K_{Fe}\rho_{Fe})^{-1} + m \sum_{i=2}^{N} \frac{m_i}{m} (\hat{K}_i\hat{\rho}_i)^{-1}, \tag{20}$$

where m_i is the mass fraction of component i, m is the total mass fraction of alloying components, $\hat{\rho}_i = w_i/\hat{V}_i$ is the effective density of component i, where w_i is its molar weight, and $\hat{K}_i = -(\partial P/\partial \ln \hat{V}_i)_S$ is the effective bulk modulus of component i.

Finally, we find for the properties of the alloy fraction

$$\hat{\rho}_A = \frac{m}{\rho^{-1} - (1 - m)\rho_{Fe}^{-1}} \tag{21}$$

and

$$\hat{K}_A = \frac{m\hat{\rho}_A^{-1}}{(\rho K)^{-1} - (1 - m)(\rho_{Fe}K_{Fe})^{-1}}, \tag{22}$$

where $\hat{\rho}_A$ and $\hat{K}_A$ are the average density and bulk modulus of the alloying constituents

$$\hat{\rho}_A^{-1} = \sum_{i=2}^{N} \frac{m_i}{m} \rho_i^{-1} \qquad \hat{K}_A^{-1} = \sum_{i=2}^{N} \frac{m_i}{m} K_i^{-1}. \tag{23}$$

We have assumed that the densities and bulk moduli of the alloying constituents are not very different from each other. In these equations the unsubscripted material properties are those of the inner core, and those subscripted Fe are taken from our iron equation of state. Equations (21) and (22) have the same form as those derived by *Jeanloz* [1979] but replace the density and bulk modulus of a single component of an ideal

binary solution with the average over an arbitrary number of components in a multicomponent nonideal solution.

6.2. Nonideal Solutions

Equations (21) and (22) yield the density and bulk modulus that must be satisfied simultaneously by the alloy fraction. Because good constraints now exist on the density and bulk modulus of both the inner core and pure iron, these equations place limits on the nature of the inner core alloy. We note that these equations contain singularities; $\hat{\rho}_A$ and $\hat{K}_A$ are positive for values of m such that

$$m > 1 - \frac{\rho_{Fe}}{\rho} \tag{24}$$

and

$$m > 1 - \frac{\rho_{Fe}K_{Fe}}{\rho K}, \tag{25}$$

respectively. While negative values of $\hat{\rho}_A$ and $\hat{K}_A$ are not strictly forbidden on thermodynamic grounds, this would require that the volume of mixing be comparable in magnitude to the molar volume itself. If we assume that $\hat{\rho}_A$ and $\hat{K}_A$ are positive, (24) and (25) set lower bounds on the mass fraction of alloying elements in the inner core. The lower bound depends on temperature through its effect on ρ_{Fe} (thermal expansion) and K_{Fe}. Calculations for a pressure of 345 GPa, the mean pressure of the inner core, show that the greatest lower bound is set by the bulk modulus equation (25) for all temperatures of interest. The lower bound only exceeds zero for the highest temperatures of our study (near 8000 K) (Figure 6).

The required properties of the alloy fraction depend on its abundance (Figure 7). Because pure iron is denser than the inner core, the effective density of the alloy fraction vanishes as its mass fraction vanishes. As the alloy mass fraction approaches unity, the required properties approach those of the inner core. The required bulk modulus diverges as the limit (25) is approached. This means in practice that the singularity
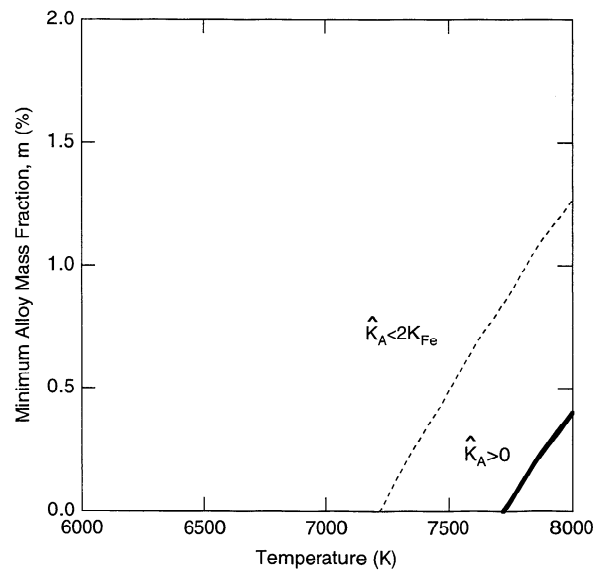

Figure 6. Lower bounds on the mass fraction of alloying components in the inner core imposed by the inequality (25) (solid line) and by the assumption that the bulk modulus of the alloy fraction is less than twice that of iron (dashed line).

in (22) places somewhat more stringent limits on the minimum allowable alloy mass fraction than the inequality (25) would suggest. For mass fractions which are as much as twice the lower bounds given by (25), the required bulk modulus of the alloy fraction is more than 3000 GPa, more than twice that of iron or of plausible alloying components. If we exclude the possibility of alloying components which have bulk moduli more than twice that of the inner core, or volumes of mixing which are comparable to molar volumes, then the smallest allowable mass fraction of alloying components according to our analysis is 1% at 8000 K (Figure 6).

6.3. Ideal Solution Approximation

If we assume that the solid solution in the inner core is ideal, then the volume of mixing is zero and we have

$$\rho_A = \hat{\rho}_A \qquad K_A = \hat{K}_A, \tag{26}$$

where ρ_A and K_A are the actual properties of the alloy fraction. Within this approximation then, we may compare our results for the required properties of the alloy fraction to those experimentally measured on several possible alloying components (Figure 7). This comparison will also allow us to test the assumption of ideality.

Empirically, nonideal behavior increases with the difference in atomic radii of the constituent species: solutions of species with similar atomic radii behave most ideally. On this basis, iron-sulfur solutions are expected to behave most ideally and to provide the most direct comparison with our results. On the other hand, there is some evidence that the Fe-S system remains eutectic to high pressures (80 GPa), implying that solid solution in this system is limited [Williams and Jeanloz, 1990]. However, even if the Fe-S system remains eutectic up to much higher pressures, the free energy gain due to the entropy of mixing due to limited amounts of solid solution would be substantial at inner core temperatures. It is likely that at least limited solid solution exists in the inner core. It is important to recall in this context that we are concerned here with limited solid solutions: the inner core is expected to contain less than 10 wt % light element. In the Fe-O system, there is some evidence from measurements of the melting curve for ideal behavior in the solid state and complete solid solution between Fe and FeO [Knittle and Jeanloz, 1991].

To estimate the properties of iron-sulfur and iron-oxygen compounds at inner core conditions, we have used the thermodynamic parameters derived from shock wave experiments on pyrite (FeS$_2$) [Ahrens and Jeanloz, 1987] and the high-pressure phases of pyrrhotite (Fe$_{0.9}$S) [Brown et al., 1984] and wüstite (FeO) [Jackson et al., 1990] (Table 3). The sulfides are expected to melt along the Hugoniot at pressures of 110 and 140 GPa, respectively. This means that substantial extrapolation of the solid-phase portions of the Hugoniots is necessary. The uncertainties in density and bulk modulus at inner core pressures may be 5% and 10%, respectively, and are due mostly to the uncertainty inherent in the extrapolation. The properties of these components are computed along the 345 GPa isobar between the temperatures of 4000 K and 8000 K and compared with the required properties of the alloy fraction from our results under the assumption of ideal mixing in Figure 8. We determine the required mass fraction of the compound, m and the corresponding mass fraction of the light element, M. For a light element containing compound with the general formula Fe$_a$L$_b$, these two quantities are related by
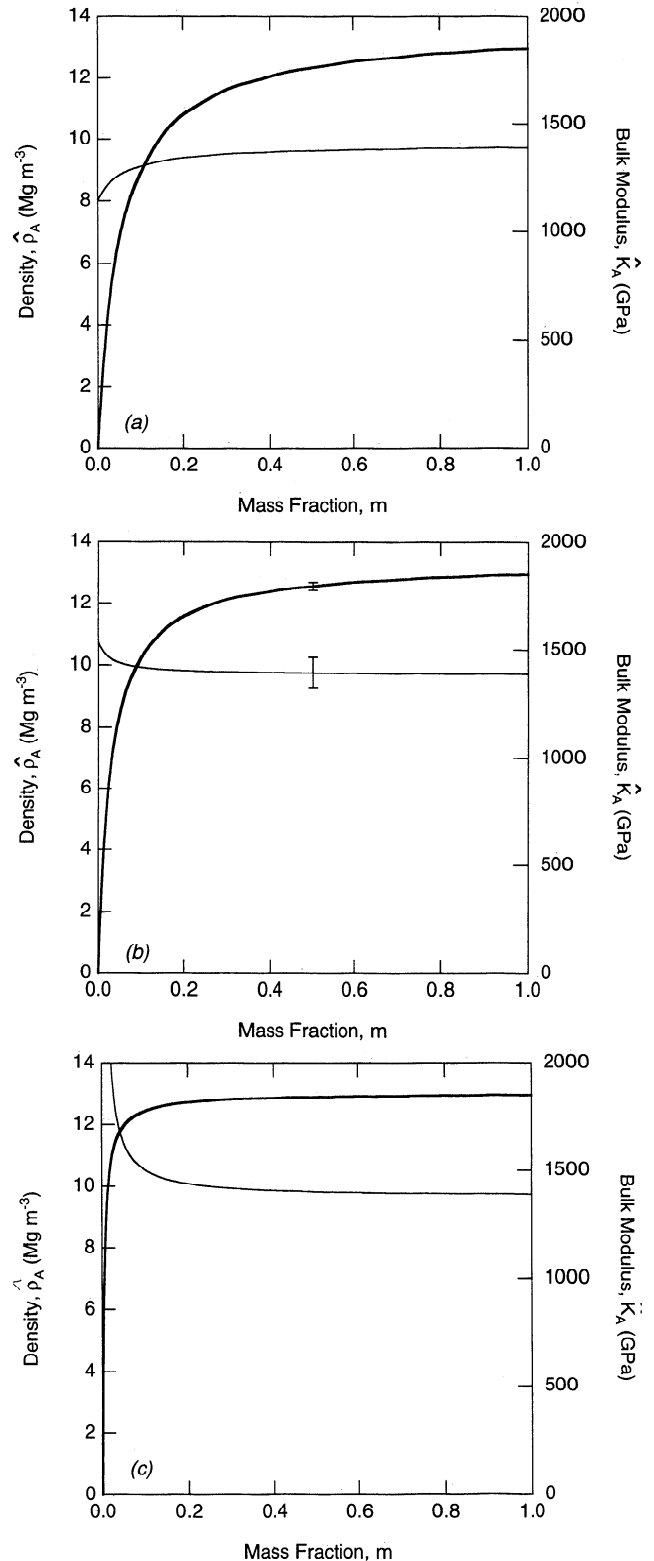

Figure 7. Properties of the alloy fraction required by the theoretical iron equation of state and seismological models of the inner core for a pressure of 345 GPa. The density and bulk modulus which must be simultaneously satisfied for a given mass fraction (m) are shown as a function of m at three different temperatures (a) 4000 K, (b) 6000 K, and (c) 8000 K. Estimated uncertainties are represented in Figure 7b (1% in density, 5% in bulk modulus).

Table 3. Equation of State Parameters of $Fe_{0.9}S$, FeS_2, and $Fe_{0.946}O$

Composition	ρ_0, Mg/m^3	K_{0S}, GPa	K'_{0S}	γ_0	β_0, J kg^{-1} K^{-2}	γ_{el}	References
$Fe_{0.9}S$	5.34	118	4.1	1.54	0.25	1.34	1, 2
FeS_2	5.01	162	4.7	1.56	0.0	· · ·	1, 3
$Fe_{0.946}O$	6.63	205	6	1.63	0.0	· · ·	4

References: 1, *Anderson and Ahrens* [1996]; 2, *Brown et al.* [1984]; 3, *Ahrens and Jeanloz* [1987]; 4, *Jackson et al.* [1990]. The parameters β_0 and γ_{el} define the electronic heat capacity $C_V^{el} = \beta_0(\rho/\rho_0)^{\gamma el}T$.

$$M = m\left(a\,\frac{w_{Fe}}{w_L} + b\right)^{-1}, \qquad (27)$$

where w_{Fe} and w_L are the molar weights of Fe and the light element, respectively.

For a given Fe-light element compound and under the assumption of ideal behavior, constraints can be placed on the temperature and alloy mass fraction required to match the properties of the inner core. The largest source of uncertainty is in the extrapolation of the solid-phase Hugoniot data. The temperature dependence of the properties of the alloy fraction according to (21) is much stronger than the temperature dependence of the density or bulk modulus of the actual compounds. Thus for ideal solutions of Fe with O as wüstite, the temperature in the inner core must lie between 6500 and 7500 K. This range of temperatures exceeds our estimate of the melting point of pure iron. It is worth pointing out, however, that addition of a light element will not necessarily depress the freezing point. Indeed, experiments indicate that the melting temperature of FeO and intermediate compounds are higher than that of pure iron [*Knittle and Jeanloz*, 1991; *Boehler*, 1992]. Ideal solutions of Fe with S require substantially lower temperatures. For S as pyrrhotite, the required temperatures are probably unrealistically low, below 4000 K. These temperatures are comparable to some estimates of the temperature at the core-mantle boundary. For S as pyrite, inner core temperatures lie between 5000 K and 6000 K. Required alloy mass fractions in the ideal solution limit are 4% FeO (1% O), >20% pyrrhotite (>8% S), and 6% pyrite (2% S).

The fact that the mass fraction of S and the required inner core temperature differ substantially depending on whether S is included as $Fe_{0.9}S$ or FeS_2 may indicate that the Fe-S solid solution at inner core conditions is substantially nonideal. The existence of nonideality in the Fe-S system is consistent with recent shock temperature measurements on iron sulfides [*Anderson and Ahrens*, 1996]. These indicate that pyrite has a strongly reduced lattice heat capacity (2/3 the Dulong Petit value) which is attributed to the survival of strong S-S bonds to high pressure. The presence of such asymmetric interactions in a binary compound would be direct evidence of nonideality. However, as Anderson and Ahrens point out, the finding of a reduced heat capacity should be approached with caution until more data are obtained. By the same token, our conclusions regarding the nonideality of the Fe-S system must be regarded as tenuous as they are based on a threefold extrapolation in pressure of the solid-phase Hugoniots. Clearly, there is a need for a better understanding of bonding in the Fe-S system at high pressure and for investigations of iron light element solutions in the iron-rich limit.

7. Discussion and Conclusions

Our theoretical equation of state of iron at high pressures and temperatures shows that the Earth's inner core is not likely

to be composed of pure iron. The alloying elements must be lighter on average than iron and have a similar bulk modulus. The amount of the noniron fraction in the inner core remains uncertain. An analysis of binary Fe-O and Fe-S mixtures under the assumption of ideal mixing indicates that the non-iron mass fraction may lie in the range $M \approx 2$–10% ($m \approx 4$–30%). The uncertainty has two important sources. First, the identity of the light element is unknown. The mass fraction of S required to satisfy seismological observations may be as much as a factor of ten greater than the required mass fraction of O. Second, the amount of S required depends on the form in which it is incorporated. The required amount of S as FeS
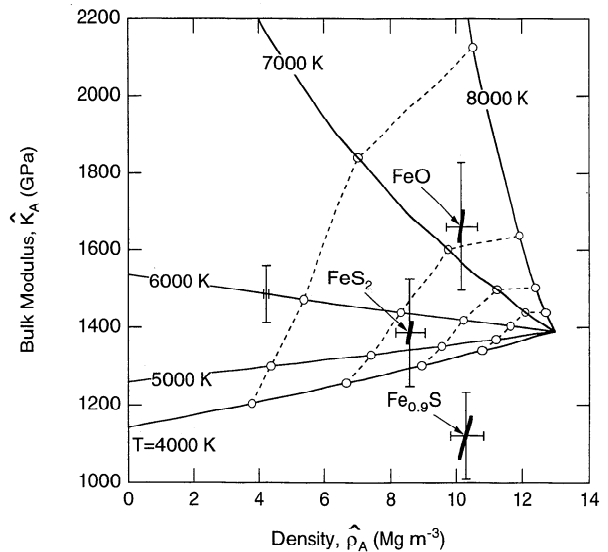

Figure 8. Properties of the alloy fraction required by the theoretical iron equation of state and seismological models of the inner core for a pressure of 345 GPa. The information conveyed by the thin solid lines is identical to that in Figure 7: for the indicated temperatures, the required effective density of the alloy fraction is plotted against its required effective bulk modulus. The symbols represent alloy mass fractions of, from left to right along a single line, 2, 5, 10, and 20%. For example, if the inner core had a temperature of 4000 K, and contained 5 wt % alloy fraction, the alloy fraction must have a density of 6.47 Mg m^{-3} and a bulk modulus of 1240 GPa. The dashed lines connect points of common mass fraction. Superimposed for comparison (bold lines) are experimentally based estimates of the properties of FeO, $Fe_{0.9}S$, and FeS_2 at 345 GPa and temperatures ranging from 4000 K (top right point of line segments) to 8000 K (bottom left point of line segments). Estimated uncertainties in the properties of these compounds are indicated: 5% in density and 10% in bulk modulus. Estimated uncertainties in the required properties of the alloy fraction are indicated on the curve corresponding to $T = 6000$ K (1% in density and 5% in bulk modulus).

differs by at least a factor of 4 from that of S as FeS_2. This difference may be caused by significant nonideality in the iron-sulfur system at inner core pressures and temperatures.

Elements heavier than iron are also likely to be present in the inner core, although their amount is uncertain. If heavier elements are present in significant amounts, the required amount of light elements would be greater than that estimated here. In the case of Ni, possibly the most abundant heavy impurity, analysis of meteorite chemistry suggests that the mass fraction of this element is 6% in the core [Birch, 1952; Ringwood, 1977]. Because its atomic weight is so similar to that of iron, addition of Ni in this amount changes the density by only 0.3%, less than the uncertainty in our theoretical equation of state or in the seismological models.

Our estimates of the amount of light element in the inner core are consistent with previous estimates of the composition of the outer core. Because of its greater density and because it is thought to form by freezing of the outer core, the inner core is expected to have a smaller abundance of alloying elements. Previous estimates of the mass fraction of O in the outer core (10% [Jeanloz and Ahrens, 1980]) are a factor of ten larger than our estimates for the inner core, while estimated abundances of S (10% [Brown et al., 1984] and 11% [Ahrens and Jeanloz, 1987]) are comparable to our highest estimate of the mass fraction of S in the inner core.

References

Ahrens, T. J., and R. Jeanloz, Pyrite: Shock compression, isentropic release, and composition of the Earth's core, *J. Geophys. Res.*, *92*, 10,363–10,375, 1987.

Anderson, O. L., *Equations of State of Solids for Geophysics and Ceramic Science*, Oxford Univ. Press, New York, 1995.

Anderson, W. W., and T. J. Ahrens, Shock temperature and melting in iron sulfides at core pressures, *J. Geophys. Res.*, *101*, 5627–5642, 1996.

Birch, F., Elasticity and composition of the Earth's interior, *J. Geophys. Res.*, *57*, 227–286, 1952.

Boehler, R., Melting of the Fe-FeO and the Fe-FeS systems at high pressure—Constraints on core temperatures, *Earth Planet. Sci. Lett.*, *111*, 217–227, 1992.

Boehler, R., Temperatures in the Earth's core from melting-point measurements of iron at high static pressures, *Nature*, *363*, 534–536, 1993.

Boness, D. A., and J. M. Brown, The electronic band structure of iron, sulfur and oxygen, *J. Geophys. Res.*, *95*, 21,721–21,730, 1990.

Boness, D. A., J. M. Brown, and A. K. McMahan, The electronic thermodynamics of iron under Earth core conditions, *Phys. Earth Planet. Inter.*, *42*, 227–240, 1986.

Brown, J. M., and R. G. McQueen, Phase transitions, Grüneisen parameter, and elasticity for shocked iron between 77 GPa and 400 GPa, *J. Geophys. Res.*, *91*, 7485–7494, 1986.

Brown, J. M., T. J. Ahrens, and D. L. Shampine, Hugoniot data for pyrrhotite and the Earth's core, *J. Geophys. Res.*, *89*, 6041–6048, 1984.

Cohen, R. E., M. J. Mehl, and D. A. Papaconstantopoulos, Tight-binding total-energy method for transition and noble metals, *Phys. Rev. B*, *50*, 14,694–14,697, 1994.

Cohen, R. E., L. Stixrude, and E. Wasserman, Elastic anisotropy at high pressure in Fe, Si, and Xe, *Phys. Rev. B*, in press, 1997.

Cowley, E. R., J. Gross, Z. X. Gong, and G. K. Horton, *Phys. Rev. B*, *42*, 3135–3141, 1990.

Dziewonski, A. M., and D. L. Anderson, Preliminary reference Earth model, *Phys. Earth Planet. Inter.*, *25*, 297–356, 1981.

Dziewonski, A. M., A. L. Hales, and E. R. Lapwood, Parametrically simple Earth models consistent with geophysical data, *Phys. Earth Planet. Inter.*, *10*, 12–48, 1975.

Holt, A. C., and M. Ross, Calculations of the Grüneisen parameter for some models of the solid, *Phys. Rev. B*, *1*, 2700–2705, 1970.

Holt, A. C., W. G. Hoover, S. G. Gray, and D. R. Shortle, Comparison of the lattice-dynamics and cell-model approximations with Monte-Carlo thermodynamic properties, *Physica*, *49*, 61–76, 1970.

Jackson, I., et al., Elasticity, shear-mode softening and high-pressure polymorphism of wüstite $(Fe_{1-x}O)$, *J. Geophys. Res.*, *95*, 21,671–21,685, 1990.

Jeanloz, R., Properties of iron at high pressures and the state of the core, *J. Geophys. Res.*, *84*, 6059–6069, 1979.

Jeanloz, R., The nature of the Earth's core, *Annu. Rev. Earth Planet. Sci.*, *18*, 357–386, 1990.

Jeanloz, R., and T. J. Ahrens, Equations of state of FeO and CaO, *Geophys. J. R. Astron. Soc.*, *62*, 505–528, 1980.

Jeanloz, R., and H.-R. Wenk, Convection and anisotropy of the inner core, *Geophys. Res. Lett.*, *15*, 72–75, 1988.

Jephcoat, A., and P. Olson, Is the inner core of the Earth pure iron, *Nature*, *325*, 332–335, 1987.

Jephcoat, A., H. K. Mao, and P. M. Bell, Static compression of iron to 78 GPa with rare gas solids as pressure-transmitting media, *J. Geophys. Res.*, *91*, 4677–4686, 1986.

Knittle, E., and R. Jeanloz, The high-pressure phase diagram of $Fe_{0.94}O$: A possible constituent of the Earth's core, *J. Geophys. Res.*, *96*, 16,169–16,180, 1991.

Mao, H. K., Y. Wu, L. C. Chen, J. F. Shu, and A. P. Jephcoat, Static compression of iron to 300 GPa and $Fe_{0.8}Ni_{0.2}$ alloy to 260 GPa: Implications for composition of the core, *J. Geophys. Res.*, *95*, 21,737–21,742, 1990.

Masters, T. G., and P. M. Shearer, Summary of seismological constraints on the structure of the Earth's core, *J. Geophys. Res.*, *95*, 21,691–21,695, 1990.

Morelli, A., and A. M. Dziewonski, Body wave traveltimes and a spherically symmetric P- and S-wave velocity model, *Geophys. J. Int.*, *112*, 178–194, 1993.

Perdew, J. P., and Y. Wang, Accurate and simple analytic representation of the electron-gas correlation energy, *Phys. Rev. B*, *45*, 13,244–13,249, 1992.

Poirier, J. P., Light elements in the Earth's outer core: A critical review, *Phys. Earth Planet. Inter.*, *85*, 319–337, 1994.

Ree, F. H., and A. C. Holt, Thermodynamic properties of the alkali-halide crystals, *Phys. Rev. B*, *8*, 826–842, 1973.

Ringwood, A. E., Composition of the core and implications for the origin of the Earth, *Geochem. J.*, *11*, 111–135, 1977.

Stixrude, L., and R. E. Cohen, Constraints on the crystalline structure of the inner core—Mechanical instability of bcc iron at high pressure, *Geophys. Res. Lett.*, *22*, 125–128, 1995a.

Stixrude, L., and R. E. Cohen, High pressure elasticity of iron and anisotropy of Earth's inner core, *Science*, *267*, 1972–1975, 1995b.

Stixrude, L., R. E. Cohen, and D. J. Singh, Iron at high pressure: Linearized-augmented-plane-wave computations in the generalized-gradient approximation, *Phys. Rev. B*, *50*, 6442–6445, 1994.

Wallace, D. C., *Thermodynamics of Crystals*, John Wiley, New York, 1972.

Wasserman, E., L. Stixrude, and R. E. Cohen, Thermal properties of iron at high pressures and temperatures, *Phys. Rev. B*, *53*, 8296–8309, 1996.

Westera, K., and E. R. Cowley, Cell-cluster expansion for an anharmonic solid, *Phys. Rev. B*, *11*, 4008–4016, 1975.

Williams, Q., and R. Jeanloz, Melting relations in the iron-sulfur system at ultra-high pressures: Implications for the thermal state of the Earth, *J. Geophys. Res.*, *95*, 19,299–19,310, 1990.

Williams, Q., R. Jeanloz, J. Bass, B. Svendsen, and T. J. Ahrens, The melting curve of iron to 250 gigapascals: A constraint on the temperature at Earth's center, *Science*, *236*, 181–182, 1987.

Yoo, C. S., et al., Shock temperatures and melting of iron at Earth core conditions, *Phys. Rev. Lett.*, *70*, 3931–3934, 1993.

R. E. Cohen, Geophysical Laboratory, 5251 Broad Branch Rd. N. W., Washington, DC 20015-1305.

L. Stixrude, Department of Geological Sciences, 2534 C. C. Little Building/425 East Univ. Ave., University of Michigan, Ann Arbor, MI 48109-1063 (e-mail: stixrude@umich.edu)

E. Wasserman, 3200 Q Ave., ETB-K9-77 Battelle, Pacific Northwest National Laboratory, Richland, WA 99352.